

**Effects of first-generation in utero exposure to diesel engine exhaust on
second-generation placental function, fatty acid profiles and foetal metabolism
in rabbits: preliminary results**

Delphine Rousseau-Ralliard^{1,2¶*}, Sarah A. Valentino^{1,2¶}, Marie-Christine Aubrière^{1,2}, Michèle Dahirel^{1,2}, Marie-Sylvie Lallemand^{1,2}, Catherine Archilla¹, Luc Jouneau¹, Natalie Fournier^{3,4}, Christophe Richard^{1,2}, Josiane Aioun^{1,2}, Anaïs Vitorino Carvalho¹, Lecardonnell Jérôme⁵, Rémy Slama⁶, Véronique Duranthon¹, Flemming R. Cassee^{7,8}, Pascale Chavatte-Palmer^{1,2¶}, Anne Couturier-Tarrade^{1,2¶*}

¹ UMR BDR, INRA, ENVA, Université Paris Saclay, Jouy en Josas, France

² PremUp Foundation, Paris, France

³ Univ. Paris-Sud, EA 4041/4529 Lip (Sys)2, UFR de Pharmacie, Châtenay-Malabry, France

⁴ Hôpital Européen Georges Pompidou (AP-HP), Laboratoire de Biochimie, UF Cardio-Vasculaire, Paris, France

⁵ GABI CRB GADIE, INRA, Université Paris Saclay, Jouy en Josas, France

⁶ Inserm, Univ. Grenoble Alpes, CNRS, IAB joint Research Center, Team of Environmental Epidemiology Applied to Reproduction and Respiratory Health, Grenoble, France

⁷ Centre for Sustainability, Environment and Health, National Institute for Public Health and the Environment, Bilthoven, Netherlands

⁸ Institute of Risk Assessment Sciences, Utrecht University, Utrecht, Netherlands.

* **Corresponding author.**

E-mail: delphine.rousseau@inra.fr and anne.couturier-tarrade@inra.fr

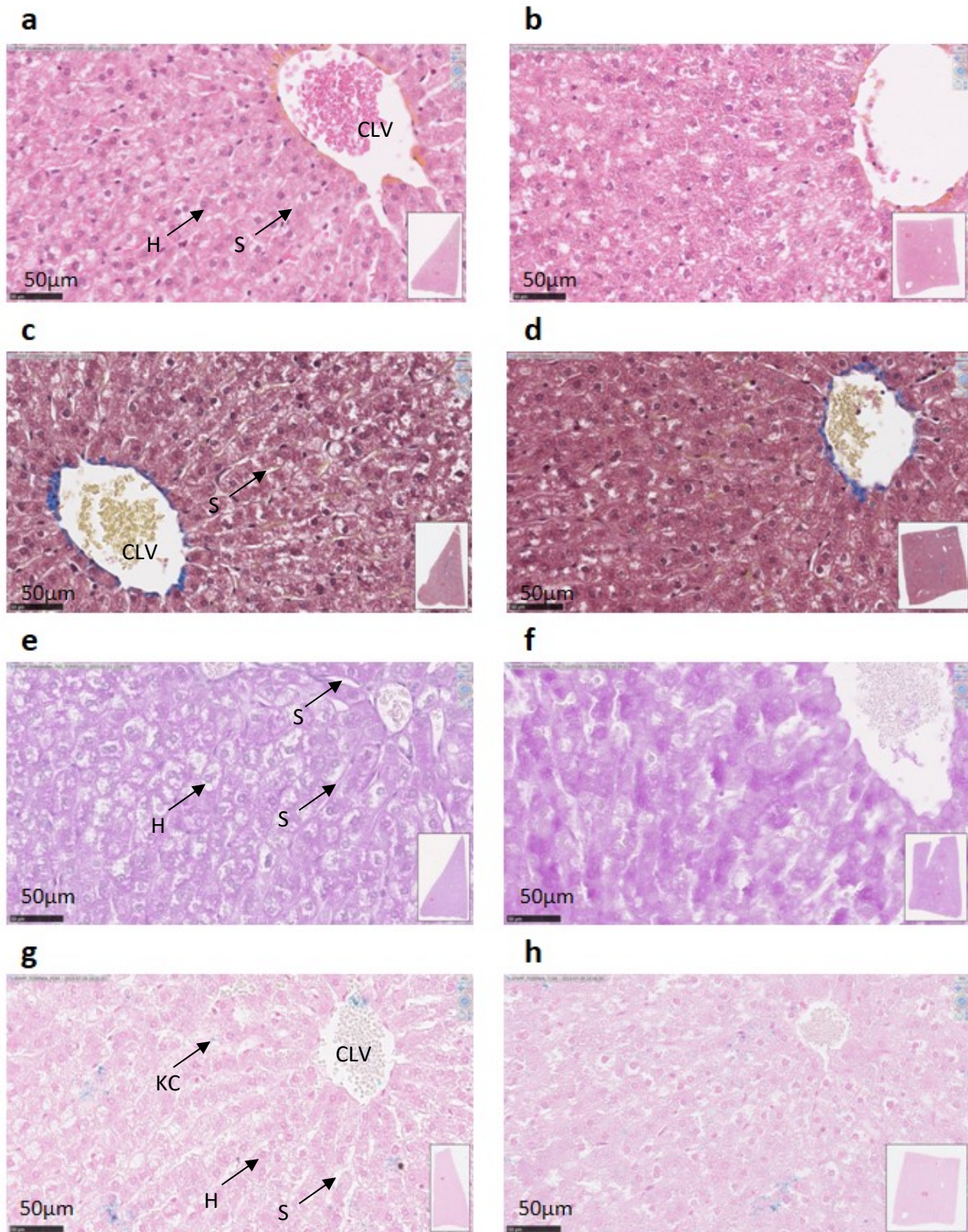
¶ The co-first Author Sarah A. Valentino has provided equal contribution as the first author.

Supplementary information online

Supplementary note: Fatty acid nomenclature

symbol	Systematic name	Trivial name
C14:0	Tetradecanoic acid	Myristic acid
C14:1	cis-9-Tetradecenoic acid	Myristoleic acid
C15:0	Pentadecanoic acid	Pentadecanoic acid
C15:1	cis-10-Pentadecenoic acid	Pentadecenoic acid
C16:0	Hexadecanoic acid	Palmitic acid
C16:1n-7	cis-9-Hexadecenoic acid	Palmitoleic acid
C18:0	Octadecanoic acid	Stearic acid
C18:1n-9	cis-9-Octadecenoic acid	Oleic acid
C18:1n-7	cis-11-Octadecenoic acid	Vaccenic acid
C18:2n-6	trans,cis-10,12-Octadecadienoic acid	Linoleic acid (LA)
C18:3n-6	cis,cis,cis-6,9,12-Octadecatrienoic acid	Gamma-linolenic acid (GLA)
C18:3n-3	cis,cis,cis-9,12,15-Octadecatrienoic acid	Alpha-linolenic acid (ALA)
C20:0	Eicosanoic acid	Arachidic acid
C20:1n-9	cis-9-Icosenoic acid	Gadoleic acid
C20:2n-6	cis-11,14-Eicosadienoic acid	Eicosadienoic acid
C20:3n-6	cis-8,11,14-Eicosatrienoic acid	Dihomo- γ -linolenic acid (DGLA)
C20:4n-6	cis,cis,cis,cis-5,8,11,14-Icosatetraenoic acid	Arachidonic acid (AA)
C20:5n-3	cis,cis,cis,cis,cis-5,8,11,14,17-Icosapentaenoic acid	Timnodonic acid (EPA)
C22:0	Docosanoic acid	Behenic acid
C22:1n-9	cis-13-Docosenoic acid	Erucic acid
C22:4n-6	cis,cis,cis,cis-7,10,13,16-Docosatetraenoic acid	Adrenic acid
C22:5n-6	cis,cis,cis,cis,cis-4,7,10,13,16-Docosapentaenoic acid	Osbond acid
C22:5n-3	cis,cis,cis,cis,cis-4,8,12,15,19-Docosapentaenoic acid	Cuplanodonic acid (DPA)
C22:6n-3	cis,cis,cis,cis,cis,cis-4,7,10,13,16,19-Docosahexaenoic acid	Cervonic acid (DHA)
C24:0	Tetracosanoic acid	Lignoceric acid
C24:1n-9	cis-15-Tetracosenoic acid	Nervonic acid

Supplementary figures online



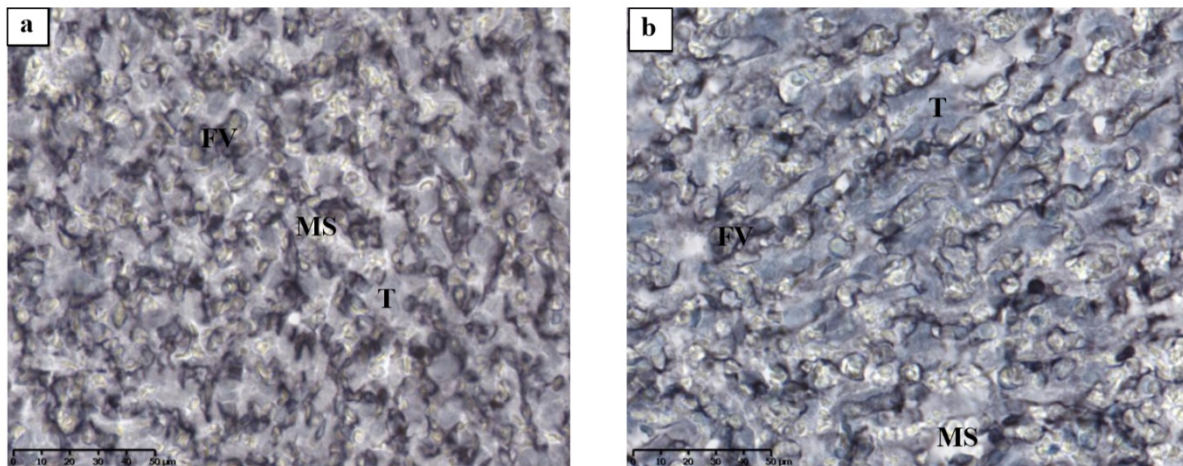
Supplementary Figure S1 online: Histological analyses of F1 maternal liver.

5µm thick sections of liver slices from *in utero* exposed F1 pregnant rabbits (n=6) on the left side or control F1 pregnant rabbits (n=3) on the right side. These liver sections were colored with **(a and b)** Hematoxyline Eosine Safran (HES) coloration to reveal the different cellular components, **(c and d)** a

Masson Trichrome coloration (Microm Microtech, France) to visualize collagen fibers, (**e and f**) a PAS (Periodic Acid Schiff) staining to highlight the presence of glycogen, and (**g and h**) a Prussian blue coloration (Perl's coloration) to highlight possible ferric deposits and activation of Kupffer cells (**KC**). All colored sections were analyzed under light microscopy and scanned using a Nanozoomer Digital Pathology System (NDP Scan U10074-01, Hamamatsu, Japan). At this x40 magnification, we can observe hepatic parenchyma and the arrangement of hepatocytes (**H**). They form flattened, anastomosing blades, the thickness of which is of a single cell, and between which the blood circulates slowly towards the centrilobular vein (**CLV**). The sinusoids (**S**) are bordered by a discontinuous layer of endothelial cells, which do not rest on any basement membrane and which are separated from the hepatocytes by a small space (Disse space); it drains into the lymphatic portals. The cytoplasm of hepatocytes is highly eosinophilic, due to the presence of numerous mitochondria, with very fine basophilic granulations linked to numerous free ribosomes and granular endoplasmic reticulum. The stained section with PAS shows the presence of glycogen grains, which, being polysaccharides, are PAS-positive (colored in magenta), in control sections mostly.

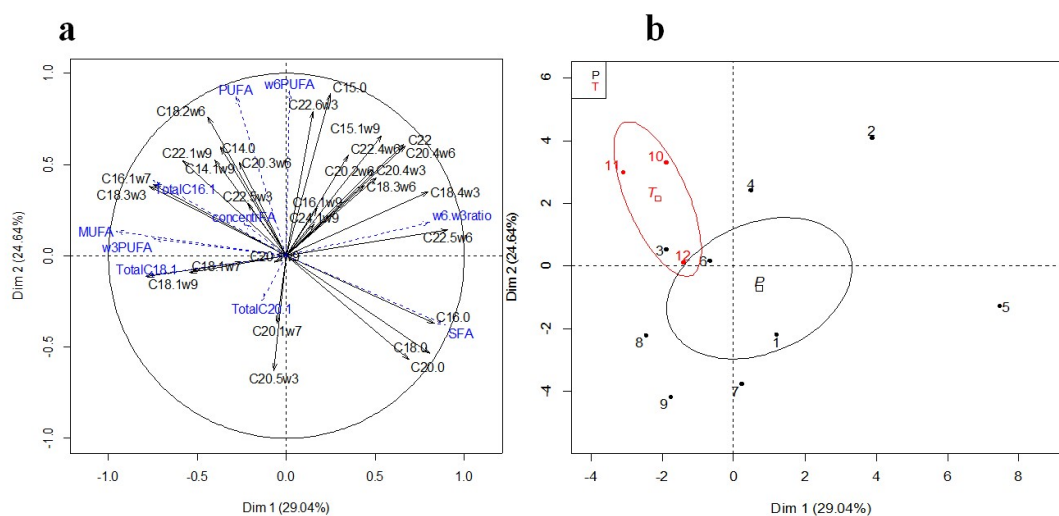
Liver sections from *in utero* exposed (E) F1 dams, once pregnant at 28 dpc, showed marked microvacuolar steatosis, with micro and macro lipid vacuoles inside hepatocytes and heterogeneous dilated sinusoids, without fibrosis (**a, c, e and g**);

Liver slice from control (C) F1 dams, once pregnant at 28 dpc, showed moderated microvacuolar steatosis (**b, d and h**) and mostly glycogen overload using PAS coloration (**f**).



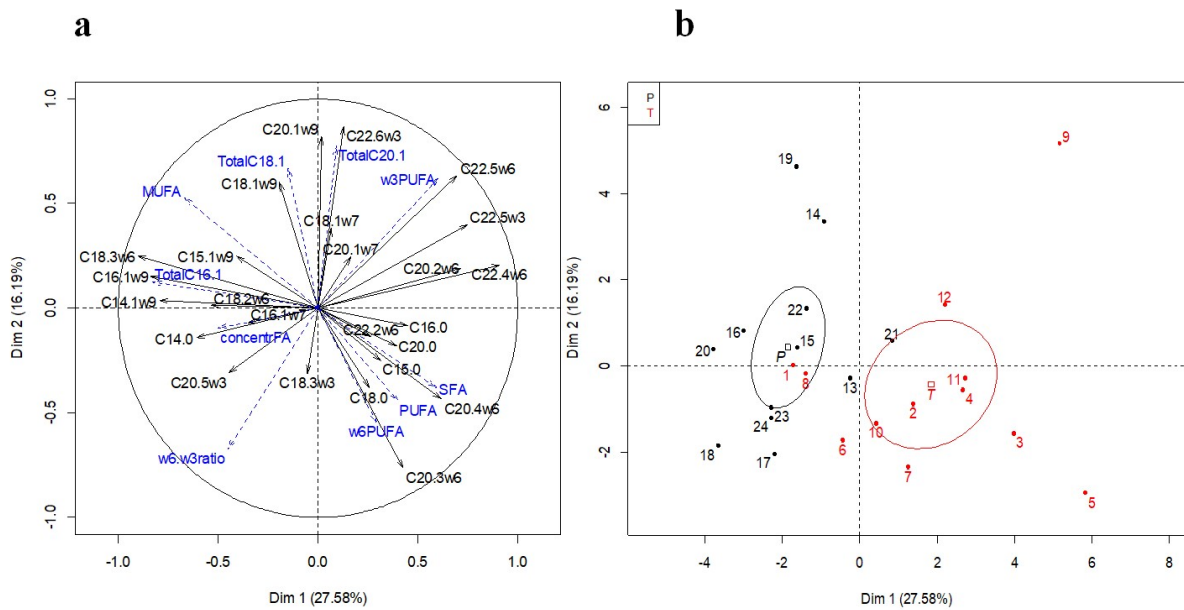
Supplementary Figure S2 online: Stereological examination of F2 placenta at 28 dpc.

At 28dpc, immunodetection of vimentin to label fetal capillaries was performed on labyrinthine area sections from the control group (a) and the exposed group (b). Black immunostaining represents fetal vessels (FV), blue cells are trophoblasts cells (T) and the white spaces with erythrocytes are maternal space (MS).



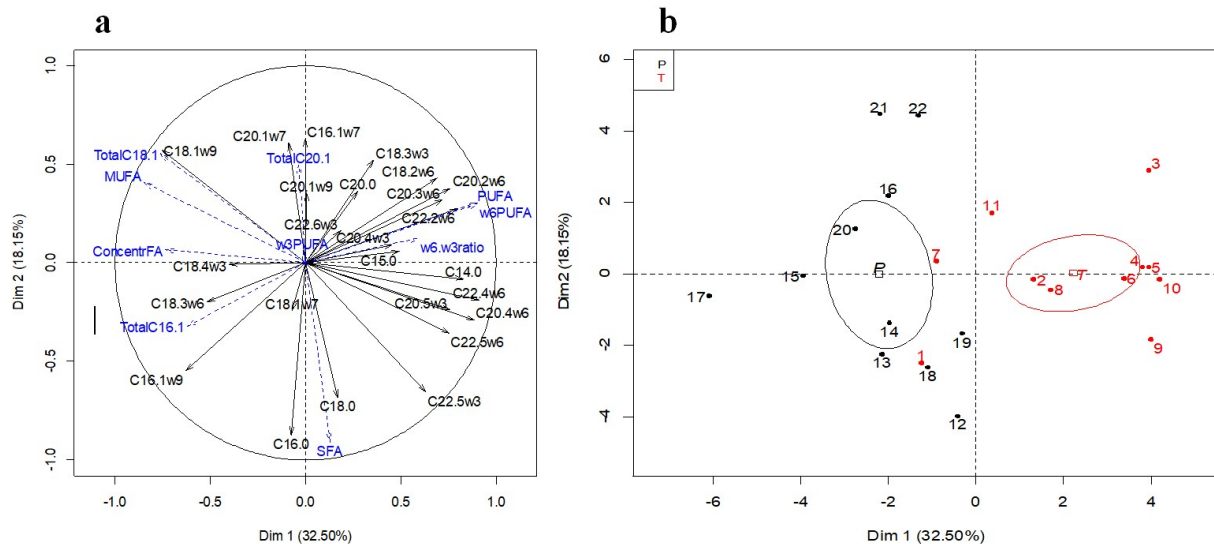
Supplementary Figure S3 online: Principal Component Analyses (PCA) of the fatty acid profile in plasma of F1 pregnant female rabbits at 28dpc.

The PCA, plotting individual factor scores, provides a representation in a space of reduced dimensions, thus providing data structure and highlighting groups of homogeneous individuals. For this, we have looked for sub-areas in which projection of the cloud deforms as little as possible the initial data summarized in Table 2: Fatty acid profiles of F1 maternal plasma (with FA expressed as % of total FA). The first principal axis is the one that maximizes the variance when data are projected onto a line and the second one is orthogonal to it, and still maximizes the remaining variance. The variables, here the fatty acids of the plasma profile, are plotted into a so-called Variables factor map (or “correlation circle” of the PCA, (a)), where the angle formed by any two variables represented as vectors, reflects their actual pairwise correlation. The Variables factor map allows identifying the variables that contribute “positively” vs. “negatively” to the PCA axes. The main plan, designed by the dimensions 1 and 2, represents 53.7% of the inertia of the data table, summarized in Table 2. The individual factor map (b) of this PCA shows that, as illustrated by the confidence ellipses drawn around the individuals, no specific FA signature characterized each group according to their *in utero* exposure, exposed (black) or control (red), since the dimension 1 does not correlate with the *in utero* treatment of the F1 female ($v.test < 2$). The main contribution of FA to dimension 1 concern a positive correlation (only the correlations >0.80 are reported here) with C22:5n-6 (0.91, $p=4.4e-05$), SFA (0.89, $p=9.88e-05$), C16:0 (0.83, $p=8.38e-04$), n-6/n-3 ratio (0.81, $p=1.57e-03$) and C18:0 (0.80, $p=1.63e-03$), and a negative correlation with MUFA (-0.96, $p=1.32e-06$). The main contributions of FA to dimension 2 concern a positive correlation with n-6 PUFA (0.90, $p=5.31e-05$), C15:0 (0.89, $p=1.09e-04$), C22:6n-3 (0.79, $p=1.97e-03$) and a negative correlation with C20:5n-3 (-0.63, $p=2.82e-02$). Using the $v.test$ from FactomineR, the statistical outputs performed on this PCA (Chi2) show nevertheless that the FA profile of plasma of the F1 Exposed female rabbits is significantly different of the control one ($p=0.034$), and that these differences are attributed to a positive association with C16:0 ($v.test=2.057$, $p=0.039$), and a negative association with C16:1n-7 ($v.test=-2.426$, $p=0.015$), C22:1n-9 ($v.test=-2.502$, $p=0.012$) and C18:3n-3 ($v.test=-2.738$, $p=0.006$), which confirm the statistical results obtained on data Table 2.



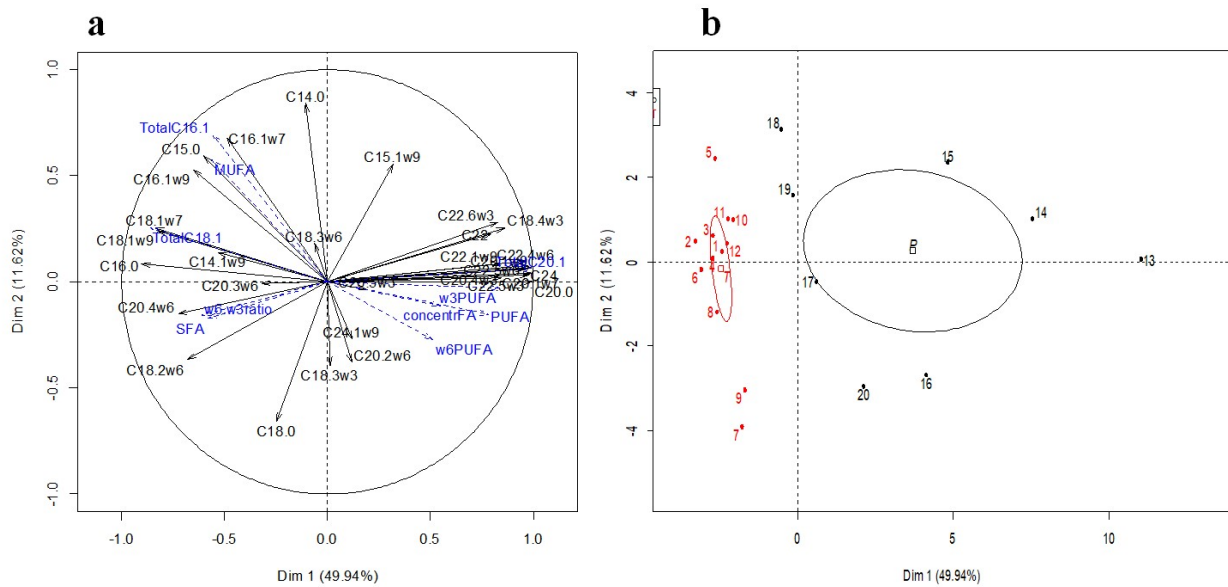
Supplementary Figure S4 online: Principal Component Analyses (PCA) of the fatty acid profile of F2 placenta phospholipids (PL) at 28dpc.

The PCA, plotting individual factor scores, provides a representation in a space of reduced dimensions, thus providing data structure and highlighting groups of homogeneous individuals. For this, we have looked for sub-areas in which projection of the cloud deforms as little as possible the initial data summarized in Table 3: Fatty acid profiles of F2 fetal plasma (with FA expressed as % of total FA). The first principal axis is the one that maximizes the variance when data are projected onto a line and the second one is orthogonal to it, and still maximizes the remaining variance. The variables, here the fatty acids of the placenta phospholipids profile, are plotted into a so-called Variables factor map (or “correlation circle” of the PCA, **A**), where the angle formed by any two variables represented as vectors, reflects their actual pairwise correlation. The Variables factor map allows identifying the variables that contribute “positively” vs. “negatively” to the PCA axes. The main plan, designed by the dimensions 1 and 2, represents 43.79% of the inertia of the data table, summarized in Table 3. The individual factor map (**B**) of this PCA shows that, as illustrated by the confidence ellipses drawn around the individuals, a specific FA signature characterized each group according to their *in utero* exposure, exposed (black) or control (red), with the dimension 1 that correlates with the *in utero* treatment of the F1 female ($v.test = -3.37$, $R^2 = 0.49$, $p = 0.0001$). The main contribution of FA to dimension 1 concern a positive correlation (only the correlations >0.70 are reported here) with C22:4n-6 (0.91, $p = 9.22e-10$), C22:5n-3 (0.75, $p = 2.83e-05$), C22:2n-6 (0.72, $p = 8.51e-05$), and a negative correlation with MUFA (-0.67, $p = 3.51e-04$) and C14:0 (-0.61, $p = 1.62e-03$). The main contribution of FA to dimension 2 concern a positive correlation with C22:6n-3 (0.87, $p = 3.35e-08$), C20:1n-9 (0.82, $p = 8.54e-07$), total C20:1 (0.78, $p = 7.94e-06$), total C18:1 (0.67, $p = 3.51e-04$), and a negative correlation with C20:3n-6 (-0.77, $p = 1.31e-05$) and n-6/n-3 ratio (-0.67, $p = 3.12e-04$). Using the $v.test$ from FactomineR, the statistical outputs performed on this PCA (χ^2) confirm that the FA profile of placental phospholipids of the F1 Exposed female rabbits is highly significantly different of the control one with a sex interaction (TS, $p = 2.50e-05$), and that these differences are attributed to a positive association with C18:3n-6 ($v.test = 3.07$, $p = 0.0021$), C16:1n-9 ($v.test = 2.59$, $p = 0.0095$), C18:2n-6 ($v.test = 2.32$, $p = 0.0204$), C14:1n-9 ($v.test = 2.16$, $p = 0.0303$), and a negative association with C22:4n-6 ($v.test = -3.61$, $p = 0.0003$), C15:0 ($v.test = -3.03$, $p = 0.0024$), C22:5n-3 ($v.test = -2.95$, $p = 0.0032$), C20:4n-6 ($v.test = -2.76$, $p = 0.0058$), C20:2n-6 ($v.test = -2.48$, $p = 0.0131$) and C22:5n-6 ($v.test = -2.05$, $p = 0.0406$).



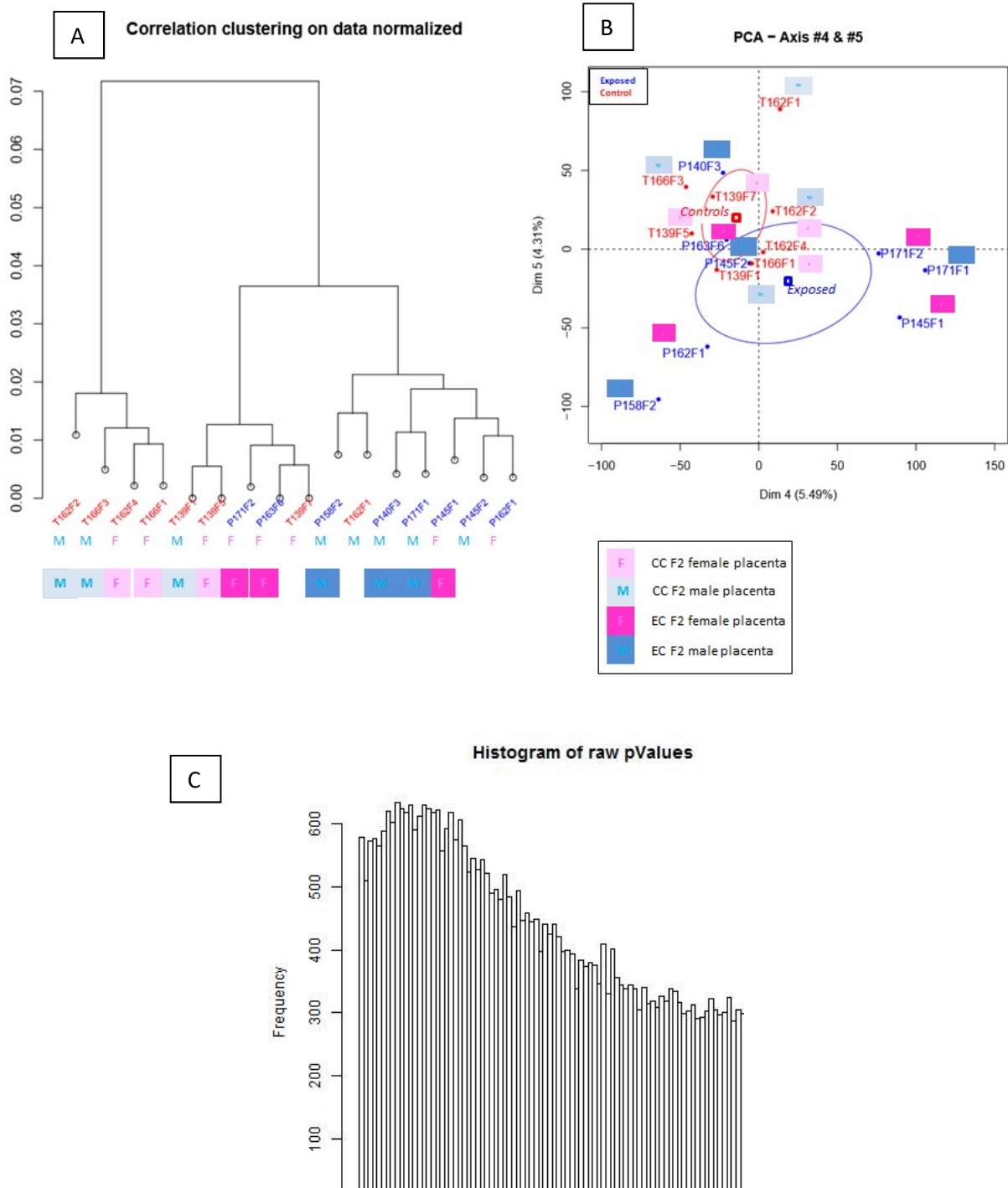
Supplementary Figure S5 online: Principal Component Analyses (PCA) of the fatty acid profile of F2 placenta neutral lipids (NL) at 28dpc.

The PCA, plotting individual factor scores, provides a representation in a space of reduced dimensions, thus providing data structure and highlighting groups of homogeneous individuals. For this, we have looked for sub-areas in which projection of the cloud deforms as little as possible the initial data summarized in Table 4: Fatty acid profiles of F2 fetal plasma (with FA expressed as % of total FA). The first principal axis is the one that maximizes the variance when data are projected onto a line and the second one is orthogonal to it, and still maximizes the remaining variance. The variables, here the fatty acids of the placenta neutral lipid profile, are plotted into a so-called Variables factor map (or “correlation circle” of the PCA, A), where the angle formed by any two variables represented as vectors, reflects their actual pairwise correlation. The Variables factor map allows identifying the variables that contribute “positively” vs. “negatively” to the PCA axes. The main plan, designed by the dimensions 1 and 2, represents 50.65% of the inertia of the data table, summarized in Table 4. The individual factor map (B) of this PCA shows that, as illustrated by the confidence ellipses drawn around the individuals, a specific FA signature characterized each group according to their *in utero* exposure, exposed (black) or control (red), with the dimension 1 that correlates with the *in utero* treatment of the F1 female (v.test = -3.57, $R^2 = 0.61$, $p = 2.00 \times 10^{-5}$). The main contribution of FA to dimension 1 concern a positive correlation (only the correlations > 0.80 are reported here) with C22:4n-6 (0.91 $p = 5.28 \times 10^{-9}$), n-6PUFA (0.90, $p = 1.20 \times 10^{-8}$), PUFA (0.88, $p = 4.58 \times 10^{-8}$), C20:4n-6 (0.88, $p = 5.56 \times 10^{-8}$), C14:0 (0.83, $p = 2.04 \times 10^{-6}$), and a negative correlation with MUFA (-0.85, $p = 7.13 \times 10^{-7}$), total C18:1 (-0.76, $p = 4.04 \times 10^{-5}$). The main contribution of FA to dimension 2 concern a positive correlation with C16:1n-7 (0.63, $p = 1.61 \times 10^{-3}$), C20:1n-7 (0.61, $p = 2.55 \times 10^{-3}$), C18:1n-9 (0.57, $p = 5.18 \times 10^{-3}$), and a negative correlation with SFA (-0.91, $p = 5.71 \times 10^{-9}$), C16:0 (-0.87, $p = 1.23 \times 10^{-7}$), and C18:0 (-0.68, $p = 4.49 \times 10^{-4}$). Using the v.test from FactomineR, the statistical outputs performed on this PCA (Chi²) confirm that the FA profile of placental NL from the F1 Exposed female rabbits is highly significantly different of the control one with a sex interaction (TS, with exposed male $>$ exposed females, $p = 5.52 \times 10^{-5}$), and that these differences are attributed to a positive association with C18:1n-9 (v.test = 3.08, $p = 0.0021$), C16:1n-9 (v.test = 2.04, $p = 0.0416$), and a negative association with C14:0 (v.test = -3.58, $p = 0.0003$), C20:4n-6 (v.test = -3.35, $p = 0.0008$), C18:2n-6 (v.test = -3.12, $p = 0.0018$), C22:4n-6 (v.test = -3.07, $p = 0.0021$), C20:5n-3 (v.test = -2.99, $p = 0.0028$), C15:0 (v.test = -2.75, $p = 0.0059$), C18:3n-3 (v.test = -2.28, $p = 0.0222$), and C20:3n-6 (v.test = -2.16, $p = 0.0305$).



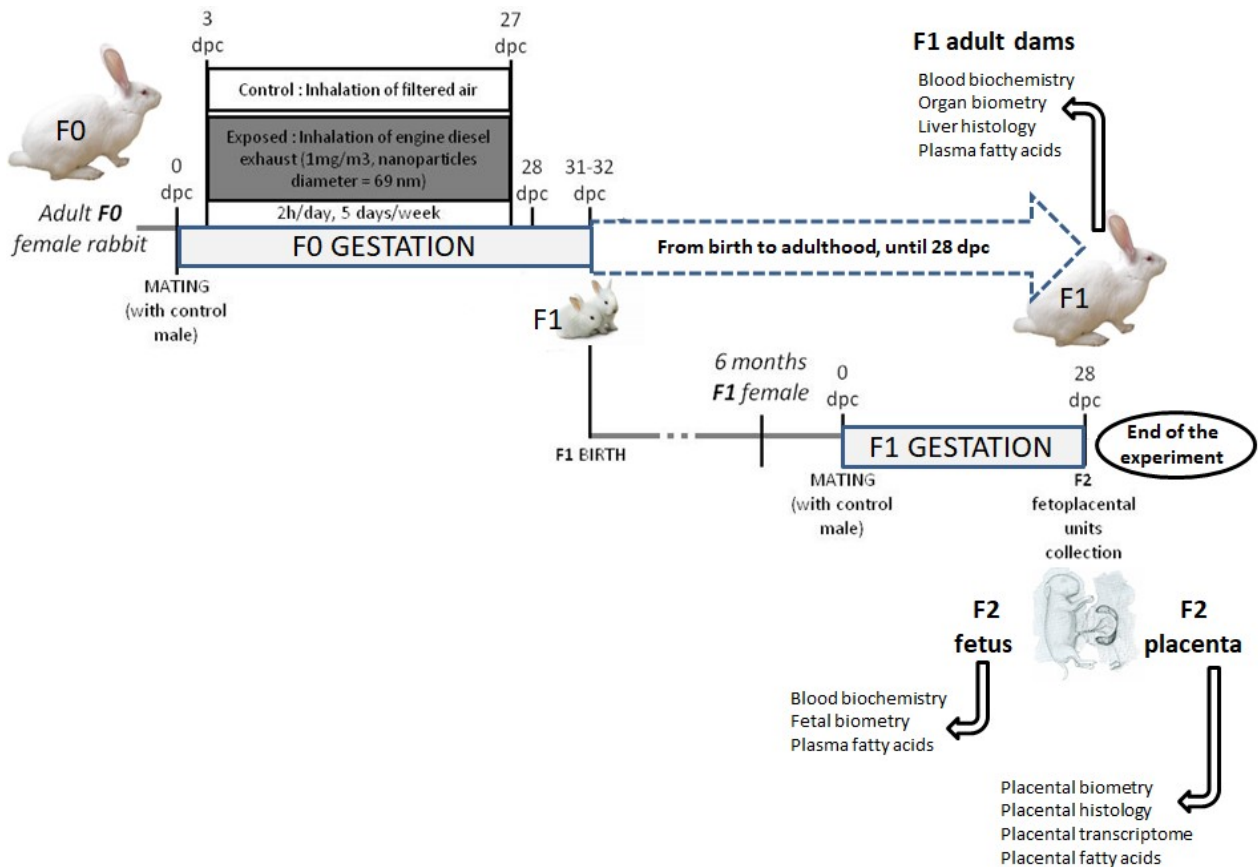
Supplementary Figure S6 online: Principal Component Analyses (PCA) of the fatty acid profile of plasma of F2 fetus at 28dpc.

The PCA, plotting individual factor scores, provides a representation in a space of reduced dimensions, thus providing data structure and highlighting groups of homogeneous individuals. For this, we have looked for sub-areas in which projection of the cloud deforms as little as possible the initial data summarized in Table 5: Fatty acid profiles of F2 fetal plasma (with FA expressed as % of total FA). The first principal axis is the one that maximizes the variance when data are projected onto a line and the second one is orthogonal to it, and still maximizes the remaining variance. The variables, here the fatty acids of the plasma profile, are plotted into a so-called Variables factor map (or "correlation circle" of the PCA, **a**), where the angle formed by any two variables represented as vectors, reflects their actual pairwise correlation. The Variables factor map allows identifying the variables that contribute "positively" vs. "negatively" to the PCA axes. The main plan, designed by the dimensions 1 and 2, represents 61.56% of the inertia of the data table, summarized in Table 6. The individual factor map (**b**) of this PCA shows that, as illustrated by the confidence ellipses drawn around the individuals, a specific FA signature characterized each group according to their *in utero* exposure, exposed (black) or control (red), with the dimension 1 that correlates with the *in utero* treatment of the F1 female ($v.test = 3.39$, $R^2 = 0.60$, $p = 5.05 \times 10^{-5}$). The main contribution of FA to dimension 1 concern a positive correlation (only the correlations > 0.80 are reported here) with C20:0 (0.99, $p = 2.73 \times 10^{-19}$), C20:1n-7 (0.99, $p = 5.16 \times 10^{-17}$), C20:1n-9 (0.99, $p = 2.30 \times 10^{-16}$), C22:5n-3 (0.97, $p = 3.40 \times 10^{-3}$), C24:0 (0.97, $p = 5.95 \times 10^{-13}$), C22:4n-6:0 (0.96, $p = 8.72 \times 10^{-12}$), C22:5n-6 (0.95, $p = 9.90 \times 10^{-11}$), C28:4n-3 (0.86, $p = 1.18 \times 10^{-6}$), and a negative correlation with C18:1n-7 (-0.84, $p = 4.32 \times 10^{-6}$), C18:1n-9 (-0.82, $p = 7.67 \times 10^{-6}$), and C20:4n-6 (-0.72, $p = 3.18 \times 10^{-4}$). The main contributions of FA to dimension 2 concern a positive correlation with C14:0 (0.84, $p = 3.35 \times 10^{-6}$) and a negative correlation with C18:0 (-0.66, $p = 1.71 \times 10^{-3}$). Using the $v.test$ from FactomineR, the statistical outputs performed on this PCA (χ^2) confirm that the FA profile of plasma of the F1 Exposed female rabbits is highly significantly different of the control one ($p = 0.006$), and that these differences are attributed to a positive association with C20:1n-7 ($v.test = 3.65$, $p = 0.0003$), C20:1n-9 ($v.test = 3.52$, $p = 0.0004$), C20:0 ($v.test = 3.48$, $p = 0.0005$), C22:0 ($v.test = 3.42$, $p = 0.0006$), C22:5n-3 ($v.test = 3.22$, $p = 0.0012$), C22:4n-6 ($v.test = 3.13$, $p = 0.0017$), and C22:1n-9 ($v.test = 3.02$, $p = 0.0025$), and a negative association with C20:4n-6 ($v.test = -3.74$, $p = 0.0018$), C18:1n-7 ($v.test = -3.59$, $p = 0.0003$), C20:3n-6 ($v.test = -2.96$, $p = 0.0031$) and C16:0 ($v.test = -2.91$, $p = 0.0036$).



Supplemental Figure S7 online. Hierarchical clustering of transcriptomes of F2 EC (noted P in blue on the graphs) and CC (noted T in red on the graphs) placentas (n=8 per condition), in rabbit.

A. Hierarchical clustering was based on the Pearson correlation coefficient of F2 EC and CC placentas transcriptome. B. Correlation circles around the groups of the Principal Component Analyses (PCA) in the plane constituted by the dimensions 4 and 5 presented here for example. Foetal sex among groups is indicated with different colours. C. Histogram of raw pValues (justifying the use of GSEA analyses).



Supplemental Figure S8 online. Experimental protocol from initial exposure of F0 females to diesel exhaust to collection of F2 fetoplacental units, in rabbit (modified from Valentino et al., PFT 2016, doi: 10.1186/s12989-016-0151-7).

Sixteen F0 females (N=7 Controls, N=9 Exposed dams) gave birth to F1 offspring, which were raised under control conditions. Altogether, 72 F1 offspring survived until adulthood, including 18 control females, 40 exposed females, 11 control males and 16 exposed males. All animals were weaned at 5 weeks of age. After becoming sexually mature adults at 6.5 months of age, a limited number of F1 nulliparous females (11 F1 control and 11 F1 exposed females) were dedicated to the production of the F2 generation. These females were mated with unexposed males. In the controls, only 5 out of 11 rabbits were diagnosed as pregnant, among which one rabbit died at mid-pregnancy and another aborted; in the exposed group 10 out of 11 rabbits were pregnant, including 1 abortion at mid-pregnancy. All females that were still pregnant (N=3 controls and N=9 exposed) were euthanized at 28 dpc to collect second generation (F2) foeto-placental units. The litter sizes were 6 to 13 fetuses without difference in sex ratio or change in fetal weight between groups.

Supplementary Tables online

Supplementary Table S1 online: Maternal biochemistry at 28dpc (control (C) or *in utero* exposed (E) F1 pregnant dams)

Variable	Number of dams		Median [Q1; Q3]		Fully adjusted linear model		
	C	E	C	E	β value	CI	p-value
Glycemia (mmol/L)	3	9	6.560 [6.020; 6.900]	5.630 [5.090; 7.070]	-0.274	[-2.145; 1.598]	0.786
Insulin (mUI/L)	3	9	4.300 [4.190; 9.610]	2.430 [1.280; 4.650]	-2.606	[-7.367; 2.155]	0.339
Total cholesterol (mmol/L)	3	9	0.200 [0.170; 0.210]	0.190 [0.165; 0.190]	-0.004	[-0.041; 0.032]	0.820
Triglycerides (mmol/L)	3	9	0.190 [0.170; 0.220]	0.240 [0.210; 0.265]	0.157	[-0.201; 0.515]	0.434
ASAT (UI/L)	3	9	29.00 [23.00; 29.00]	35.50 [28.50; 42.00]	8.125	[-0.363; 16.61]	0.131
ALAT (UI/L)	3	9	18.00 [15.00; 20.00]	12.00 [7.500; 18.50]	-4.778	[-11.71; 2.151]	0.244
Creatinine (μ mol/L)	3	9	84.00 [83.00; 111.0]	102.0 [81.00; 109.0]	-0.095	[-27.37; 27.18]	0.995
Urea (mmol/L)	3	9	4.900 [4.200; 5.100]	4.600 [3.650; 5.350]	0.122	[-1.627; 1.871]	0.897

ASAT: Aspartate Aminotransferase; ALAT: Alanine Aminotransferase. F0 female rabbits inhaled 1mg/m³ of NPs, 2 hours/day, 5 days/week, from 3 dpc to 27dpc during gestation. Dams were allowed to give birth to the generation F1. Adult F1 female (7.5 months of age), *in utero* exposed, were mated and euthanized when pregnant at 28 dpc.

Supplementary Table S2 online: Stereological data of placenta for the second generation

Variable	Number of fetus		Median [Q1; Q3]		Fully adjusted linear model		
	CC	EC	CC	EC	β value	CI	p-value
Volume fraction of trophoblast	6	6	33.66 [28.45; 38.50]	35.20 [31.97; 41.71]	4.075	[-8.041; 16.19]	0.542
Volume fraction of fetal capillaries	6	6	22.01 [17.70; 25.79]	16.95 [12.78; 26.48]	-3.609	[-10.87; 3.649]	0.381
Volume fraction of maternal blood space	6	6	38.33 [31.71; 46.27]	38.48 [33.75; 43.00]	0.105	[-8.199; 8.408]	0.981
Surface density of trophoblast	6	6	0.252 [0.203; 0.278]	0.241 [0.179; 0.281]	-0.008	[-0.047; 0.030]	0.692
Surface density of fetal capillaries	6	6	0.248 [0.201; 0.296]	0.220 [0.188; 0.251]	-0.027	[-0.075; 0.021]	0.328
Surface density of maternal blood space	6	6	0.269 [0.244; 0.320]	0.245 [0.211; 0.276]	-0.047	[0.120; 0.026]	0.269

F0 female rabbits inhaled 1mg/m³ of NPs, 2 hours/day, 5 days/week, from 3 dpc to 27dpc during gestation. Dams were allowed to give birth to the generation F1. Adult F1 female (7.5 months of age), *in utero* exposed, were mated and euthanized when pregnant at 28 dpc. Fetoplacental units of generation F2 were collected in control (CC) and exposed (EC) groups. Placental labyrinthine was fixed in Formalin and included in paraffin for histological analysis. After preparation of histological sections with microtome, immunodetection of vimentin to label fetal capillaries was performed on labyrinthine area sections from the control group and the exposed group. Volume fraction of trophoblast, fetal capillaries and maternal blood space and surface density of fetal capillaries were quantified. Effect of grand-dam (F0) pregnancy exposure to engine diesel exhaust on second-generation fetuses was estimated using linear model with random effect of dam (F1) adjusted for number of fetuses by dam, fetus position in the horn and fetus sex. All data are expressed as median[Q1;Q3].(*p < 0.05).

Supplementary Table S3 online: Differential gene expression in transcriptomics analyses in EC versus CC placentas, normalized signal and annotated genes (cf. file in .txt format)

Supplementary Table S4 online: Gene set Enrichment Analysis - Database C2:KEGG.

Population	Pathway	Annotated gene number	Enrichment Core gene number	NES	FDR q-value
Exposed	RNA degradation	41	22	2.07	0.015
	Ubiquitin mediated proteolysis	98	40	1.96	0.033
	Protein export	16	12	1.93	0.024
	AminoacylTRNA biosynthesis	35	20	1.86	0.035
	N-Glycan biosynthesis	29	14	1.79	0.049
	Adherens Junction	62	19	1.77	0.049
	Endocytosis	125	49	1.71	0.066
	Sphingolipid metabolism	27	11	1.69	0.069
	Valine/Leucine/Isoleucine degradation	37	18	1.52	0.209
Chronic myeloid Leukemia	59	25	1.5	0.215	
Control	Olfactory transduction	82	56	-2.03	0.000
	Neuroactive ligand receptor interaction	181	127	-2.02	0.000
	Systemic lupus erythematosus	40	27	-1.87	0.009
	Allograft rejection	18	11	-1.78	0.023
	Autoimmune Thyroid disease	19	12	-1.75	0.029
	Graft versus hist disease	15	11	-1.73	0.030
	Intestinal immune network for IGA production	30	21	-1.67	0.059
	Drug metabolism other enzymes	23	8	-1.66	0.061
	Dilated cardiomyopathy	71	27	-1.54	0.163
	Cardiac muscle contraction	43	17	-1.53	0.170
	Calcium signaling pathway	130	58	-1.50	0.197
	Complement and coagulation cascades	52	35	-1.50	0.186
	Primary immunodeficiency	26	12	-1.49	0.180
	Hypertrophic cardiomyopathy HCM	68	26	-1.47	0.209
	Cell adhesion molecules cams	92	43	-1.43	0.254
Adipocytokine signaling pathway	58	21	-1.43	0.247	

FDR: False Discovery Rate; NES: Normalized Enrichment Score.

Gene set enrichment analysis (GSEA) (also known as functional enrichment analysis) is a method to identify classes of genes that are over-represented in a large set of genes, and may have an association with disease phenotypes or biological processes. The method uses statistical approaches to identify significantly enriched or depleted groups of genes. Microarray results often identify thousands of genes which are used for the analysis. Gene set enrichment analysis uses a priori gene sets that have been grouped together by their involvement in the same biological pathway. The top and bottom of the list correspond to the largest differences in expression between the two cell types or conditions. If the gene set falls at either the top (over-expressed) or bottom (under-expressed), it is thought to be related to the phenotypic differences. In the method that is typically referred to as standard GSEA, there are three steps involved in the analytical process. The general steps are summarized below: 1) Calculate the enrichment score (ES) that represents the amount to which the genes in the set are over-represented at either the top or bottom of the list. This score is a Kolmogorov–Smirnov-like statistic. 2) Estimate the statistical significance of the ES. This calculation is done by a phenotypic-based permutation test in order to produce a null distribution for the ES. 3) Adjust for multiple hypothesis testing for when a large number of gene sets are being analyzed at one time. The enrichment scores for each set are normalized and a false discovery rate is calculated.

Supplementary Table S5 online: Gene set Enrichment Analysis - Database Gene Ontology, C5:BP.

Population	Pathway	Annotated gene number	Enrichment Core gene number	NES	FDR q-value
Exposed	Golgi vesicle transport	33	16	2.22	0.012
	Phosphoinositide metabolic process	21	9	1.93	0.103
	Intracellular transport	210	54	1.89	0.094
	Endosome transport	18	7	1.87	0.085
	Ubiquitin cycle	31	14	1.82	0.096
	Protein ubiquitination	24	12	1.81	0.085
	Viral infectious cycle	22	11	1.75	0.122
	Intracellular protein transport	114	39	1.73	0.125
	Protein modification by small protein conjugation	26	13	1.68	0.158
	Phosphoinositide biosynthetic process	15	6	1.66	0.159
	Sphingolipid metabolic process	22	7	1.65	0.154
	Protein transport	122	40	1.58	0.222
	Membrane lipid metabolic process	72	21	1.56	0.248
Establishment of cellular localization	256	58	1.56	0.231	
Control	Oxygen and reactive oxygen species metabolic process	18	7	-1.78	0.219
	Development of primary sexual characteristics	19	6	-1.68	0.243
	Detection of stimulus	34	22	-1.66	0.236
	Excretion	26	13	-1.66	0.214
	Regulation of secretion	27	16	-1.65	0.199
	Negative regulation of protein metabolic process	35	14	-1.65	0.197
	Second messenger mediated signaling	106	62	-1.63	0.202
	Negative regulation of protein metabolic process	33	13	-1.62	0.211
	Metal ion transport	85	51	-1.62	0.202
	Monovalent inorganic cation transport	64	39	-1.62	0.190
	Brain development	37	22	-1.61	0.196
	System process	380	179	-1.61	0.180
	Neurological system process	259	143	-1.59	0.207
	G protein signaling coupled to cyclic nucleotide second messenger	69	41	-1.58	0.218
	Transmission of nerve impulse	125	64	-1.57	0.230
	Cyclic nucleotide mediated signaling	71	-	-1.56	0.242
Lymphocyte activation	41	-	-1.55	0.243	
Cellular defense response	31	-	-1.55	0.242	

FDR: False Discovery Rate; NES: Normalized Enrichment Score.

Supplementary Table S6 online: Gene set Enrichment Analysis - Database Gene Ontology, C5:CC.

Population	Pathway	Annotated gene number	Enrichment Core gene number	NES	FDR q-value
Exposed	Proteasome complex	18	12	2.16	0.016
	Nuclear pore	21	15	2.07	0.013
	Nuclear envelope	50	24	2.03	0.020
	Integral to organelle membrane	42	19	2.02	0.016
	Organelle membrane	207	88	1.96	0.019
	Nuclear membrane part	28	17	1.95	0.018
	Endomembrane system	158	72	1.92	0.020
	Peroxisome	35	14	1.90	0.021
	Nuclear membrane	33	18	1.89	0.020
	Intrinsic to organelle membrane	44	19	1.86	0.021
	Microbody	35	14	1.86	0.020
	Pore complex	25	15	1.84	0.021
	Golgi membrane	38	21	1.76	0.039
	Organelle envelope	110	34	1.66	0.067
	Envelope	110	34	1.65	0.066
	Endoplasmic reticulum	194	60	1.62	0.075
	DNA directed RNA polymerase II holoenzyme	42	15	1.56	0.106
	Nuclear part	388	116	1.54	0.114
Golgi Apparatus part	83	36	1.52	0.124	
Control	Extracellular matrix	79	31	-1.72	0.185
	Proteinaceous extracellular matrix	78	31	-1.71	0.097
	Spindle	30	11	-1.66	0.121
	Microtubule cytoskeleton	114	31	-1.66	0.093
	Extracellular region part	241	124	-1.66	0.075
	Collagen	22	9	-1.60	0.101
	Voltage gated potassium channel complex	23	13	-1.55	0.145
	Extracellular region	313	155	-1.53	0.145
	Extracellular space	167	99	-1.53	0.134
	Cytoskeleton	271	66	-1.46	0.199
	Cytoskeletal part	179	38	-1.45	0.208

FDR: False Discovery Rate; NES: Normalized Enrichment Score.

Supplementary Table S7 online: Gene set Enrichment Analysis - Database Gene Ontology, C5:MF.

Population	Pathway	Annotated gene number	Enrichment Core gene number	NES	FDR q-value
Exposed	Signal sequence binding	15	6	2.24	0.007
	Small protein conjugating enzyme activity	35	15	2.13	0.013
	Ubiquitin protein ligase activity	34	14	2.08	0.014
	Ligase activity forming carbon nitrogen bonds	48	17	2.08	0.013
	Cysteine type peptidase activity	43	15	2.06	0.011
	Acid/amino acid ligase activity	40	15	1.99	0.016
	Small conjugating protein ligase activity	36	14	1.98	0.016
	Cysteine type endopeptidase activity	35	14	1.76	0.077
	Ligase activity	72	23	1.65	0.139
	Hydrolase activity acting on acid anhydrides	170	66	1.65	0.130
	Coenzyme binding	15	9	1.64	0.120
	Pyrophosphatase activity	168	66	1.64	0.114
	Nucleoside triphosphate activity	157	62	1.61	0.129
	GTPase activity	62	24	1.57	0.156
RNA helicase activity	16	8	1.52	0.188	
Control	Rhodopsin like receptor activity	80	54	-1.93	0.026
	Amine receptor activity	22	16	-1.83	0.067
	Cation channel activity	81	50	-1.80	0.063
	G protein coupled receptor activity	121	77	-1.77	0.067
	G protein coupled receptor binding	31	20	-1.75	0.066
	Substrate specific channel activity	108	71	-1.73	0.071
	Ion channel activity	103	66	-1.72	0.063
	Chemokine activity	21	12	-1.62	0.156
	Chemokine receptor binding	21	12	-1.61	0.151
	Calcium channel activity	24	14	-1.61	0.148
	Gated channel activity	86	53	-1.59	0.164
	Cation transmembrane transporter activity	154	53	-1.58	0.162
	Voltage gated cation channel activity	45	31	-1.57	0.163
	Voltage gated channel activity	49	33	-1.55	0.185
	Cytokine activity	66	32	-1.54	0.191
	Ion transmembrane transporter activity	203	64	-1.53	0.195
	Transmembrane receptor activity	277	137	-1.51	0.211
	Hormone activity	31	14	-1.50	0.211
	Pattern binding	29	19	-1.49	0.214
	Metal ion transmembrane transporter activity	104	62	-1.48	0.221
Protein C terminus binding	50	-	-1.48	0.225	
Extracellular matrix structural constituent	20	-	-1.47	0.225	
Receptor binding	266	-	-1.46	0.225	
Motor activity	21	-	-1.46	0.217	

FDR: False Discovery Rate; NES: Normalized Enrichment Score.